

**A Statistical Forecast Model for Atlantic Seasonal Hurricane Activity Based on the  
NCEP Dynamical Seasonal Forecast**

HUI WANG<sup>1,2</sup>, JAE-KYUNG E. SCHEMM<sup>1</sup>, ARUN KUMAR<sup>1</sup>, WANQIU WANG<sup>1</sup>  
LINDSEY LONG<sup>1,2</sup>, MUTHUVEL CHELLIAH<sup>1</sup>, GERALD D. BELL<sup>1</sup>, and PEITAO PENG<sup>1</sup>

<sup>1</sup>*Climate Prediction Center, NCEP/NWS/NOAA, Camp Springs, Maryland*

<sup>2</sup>*Wyle Information Systems, McLean, Virginia*

Journal of Climate  
Manuscript submitted 25 July 2008  
Revised 22 January 2009

*Corresponding author address:* Dr. Hui Wang, NOAA Climate Prediction Center,  
5200 Auth Road, Camp Springs, MD 20746.  
E-mail: hui.wang@noaa.gov

## ABSTRACT

A statistical forecast model is developed for predicting Atlantic seasonal hurricane activity. The model is built upon the empirical relationship between the observed interannual variability of hurricanes and the variability of sea surface temperatures (SSTs) and vertical wind shear in 26-yr (1981–2006) hindcasts from the National Centers for Environmental Prediction (NCEP) Climate Forecast System (CFS).

The number of Atlantic hurricanes exhibits large year-to-year fluctuations and an upward trend over the 26 years. The latter is characterized by an inactive period prior to 1995 and an active period afterwards. The interannual variability of the Atlantic hurricanes significantly correlates with the CFS hindcasts for August–September–October (ASO) SSTs and vertical wind shear in the tropical Pacific and tropical North Atlantic where CFS also displays skillful forecasts for the two variables. In contrast, the hurricane trend shows less of a correlation to the CFS predicted SSTs and vertical wind shear in the two tropical regions. Instead, it strongly correlates with observed pre-season SSTs in the far North Atlantic. Based on these results, three potential predictors for the interannual variation of seasonal hurricane activity are constructed by averaging SSTs over the tropical Pacific (TPCF; 170°E–130°W, 5°S–5°N) and the Atlantic hurricane Main Development Region (MDR; 20°W–80°W, 10°N–20°N), respectively, and vertical wind shear over the MDR, all of which are from the CFS dynamical forecasts for the ASO season. In addition, two methodologies are proposed to better represent the *long-term trend* in the number of hurricanes. One is the use of observed pre-season SSTs in the North Atlantic (NATL; 30°W–60°W, 55°N–65°N) as a predictor for the hurricane trend, and the other is the use of a step function that breaks up the hurricane climatology into a

generally inactive period (1981–1994) and a very active period (1995–2006). The combination of the three predictors for the interannual variation, along with the two methodologies for the trend, is explored in developing an empirical forecast system of the Atlantic hurricanes.

A cross-validation of the hindcasts for the 1981–2006 hurricane seasons suggests that the seasonal hurricane forecast with the TPCF SST as the only CFS predictor is more skillful in inactive hurricane seasons, while the forecast with only the MDR SST is more skillful in active seasons. The forecast using both predictors gives better results. The most skillful forecast uses the MDR vertical wind shear as the only CFS predictor. A comparison with forecasts made by other statistical models over the 2002–2007 seasons indicates that this hybrid dynamical-statistical forecast model is competitive with the current statistical forecast models.

## 1. Introduction

Atlantic hurricane activity has increased markedly since 1995 (Zehr and Knaff 2007). Some studies attribute this increase to global warming (Emanuel 2005; Webster et al. 2005), while others tie it to the natural variability on multidecadal time scales, the so-called Atlantic Multidecadal Oscillation (AMO; Enfield et al. 2001; Goldenberg et al. 2001; Bell and Chelliah 2006). Regardless of cause, most researches (Saunders and Lea 2008) relate the increase of Atlantic hurricane activity since the mid 1990s to considerable warming in tropical Atlantic sea surface temperatures (SSTs), along with reduced vertical wind shear in the Atlantic hurricane Main Development Region (MDR; 20°W–80°W, 10°N–20°N). In addition to the long-term change, the number of hurricanes also fluctuates considerably from year to year. For example, the 2005 Atlantic hurricane season ranked as the most active season in recorded history with 15 hurricanes, while the 1982 season only had two.

The significant variability of Atlantic hurricanes on different time scales is also accompanied by variability in the atmosphere and oceans (Goldenberg and Shapiro 1996; Goldenberg et al. 2001). Figure 1 shows the number of hurricanes during the Atlantic hurricane season (June–November) from 1981 to 2006 and the August–September–October (ASO) seasonal mean anomalous SSTs and vertical shear of zonal wind between 200 and 850 hPa averaged over the MDR. The observational data in Fig. 1 are taken from the National Oceanic and Atmospheric Administration (NOAA) Hurricane Best Track Database (Landsea et al. 2004), the NOAA optimum interpolation SST version 2 (OISST v2; Reynolds et al. 2002) and the National Centers for Environmental Prediction (NCEP) – Department of Energy (DOE) Reanalysis 2 (R2; Kanamitsu et al. 2002). The

number of hurricanes, MDR SST and the negative vertical wind shear exhibit coherent interannual variations, as well as an upward trend. The correlation between the hurricane variability and the MDR SST is 0.66 and the correlation to the wind shear is  $-0.69$ , consistent with the well-known fact that an active hurricane season is associated with warm Atlantic SSTs and weak wind shear (Goldenberg et al. 2001).

Apart from local climate factors, the El Niño–Southern Oscillation (ENSO) is also known to remotely influence the Atlantic hurricane activity through changes in vertical wind shear that extend beyond the MDR (Gray 1984a; Goldenberg and Shapiro 1996; Bengtsson et al. 2007). For example, the three inactive seasons of 1982, 1987 and 1997, all of which are El Niño years, show no apparent local SST and MDR wind shear anomalies that would indicate low seasonal hurricane activity (Fig. 1). This evidence that seasonal hurricane activity is influenced by multiple factors poses a challenge in quantifying the contribution to the total seasonal hurricane activity from various components.

Since 1984 when Grey (1984a,b) first attempted to make forecasts of Atlantic hurricane activity for the upcoming season at Colorado State University (CSU), considerable improvements have been made (Hess and Elsner 1994; Klotzbach 2007), including the availability of hurricane outlooks from multiple sources. For example, seasonal hurricane outlooks have now been issued at NOAA operationally since 1999. Despite recent advances, however, most of the current seasonal hurricane forecast methods are still statistical in nature with various predictors representing different local and remote influences. The CSU forecast methodology, for example, uses preseason SSTs in the North Atlantic, 500-hPa height over Greenland, and sea level pressure in the

subtropical central Pacific to issue 6-month lead forecasts of seasonal hurricane activity (Klotzbach and Gray 2007), while NOAA outlooks issued in the middle of May and early August rely more on the anticipated state of ENSO and current phase of the AMO (NOAA 2007).

A common feature of the observational based statistical forecasts is the use of the lagged relationship between seasonal hurricane activity and preseason atmosphere and ocean conditions. With the development of dynamical seasonal forecast systems in the last decade (e.g., Ji et al. 1994; Mason et al. 1999; Alves, et al. 2002; Kanamitsu et al. 2002; Palmer et al. 2004), the possibility now exists that model-based predictions of large-scale variables can be used as a set of predictors in the statistical hurricane forecast schemes. Development of such an approach is the focus of this paper.

As an alternate to the model based statistical approach, seasonal hurricane outlooks from the direct count of storm systems can also be pursued (Vitart and Stockdale 2001; Vitart et al. 2007). In the present analysis, however, we only focus on the feasibility of utilizing dynamical prediction of large-scale variability of the atmosphere and oceans for seasonal hurricane forecasts because (1) observational analysis indicates a strong relationship between the interannual hurricane activity and large-scale variability (Fig. 1), and (2) the dynamical seasonal forecast system used in this analysis, i.e., the Climate Forecast System (CFS) operational at NCEP, is a low resolution seasonal forecast system and seasonal hurricane predictions based on direct counts is not feasible. Further, even with the development of higher resolution seasonal prediction models, statistical prediction based on model predictors is still a viable and complementary approach.

The skillful prediction of large-scale atmosphere and ocean variability with the CFS (Saha et al. 2006), together with the evidence of strong association between seasonal hurricane activity and ASO Atlantic/Pacific SSTs and local wind shear (Fig. 1), is the primary basis for the use of predictive information from the CFS seasonal forecasts in predicting the Atlantic seasonal hurricane activity. The variability of both the tropical Pacific and Atlantic SSTs, as well as the associated change in local wind shear, have been identified as the primary sources of variation in hurricane activity in many previous studies (e.g., Gray 1984a; Goldenberg and Shapiro 1996; Goldenberg et al. 2001). Therefore, these three predictors are considered in this study. We will show that with limited predictors derived from the CFS dynamical seasonal forecasts, the prediction of seasonal hurricane activity is as skillful as current empirical forecast models (e.g., Klotzbach and Gray 2007).

This paper is organized as follows. Section 2 provides a brief description of the datasets used and both analysis and prediction methods. Section 3 examines CFS predictive skill for SSTs and vertical wind shear. The observed variability of Atlantic hurricanes and its relation to local Atlantic SSTs and vertical wind shear, as well as remote tropical Pacific SSTs, are assessed in section 4. The predictability of the seasonal hurricane activity based on the CFS forecasts of large-scale atmosphere and ocean conditions is discussed in section 5. Conclusions are given in section 6.

## **2. Data and methods**

The observational data used in this study include the actual number of Atlantic hurricanes occurring during the Atlantic hurricane season, monthly mean SSTs and zonal wind at 200 and 850 hPa. Although the Atlantic hurricane season begins on June 1st and

ends on November 30th, 90% of hurricanes occur during the three months of ASO, the heart of the Atlantic hurricane season. Therefore, similar to many previous studies (e.g., Bell and Chelliah 2006; Knutson et al. 2007), our analysis of the atmospheric wind and SSTs focuses on the ASO season. The hurricane data are from the NOAA Hurricane Best Track Database (Landsea et al. 2004). The observational SST and wind data covering a 26-yr period (1981–2006) are from the NOAA optimum interpolation SST version 2 (OISST v2; Reynolds et al. 2002) and the NCEP–DOE Reanalysis 2 (R2; Kanamitsu et al. 2002), on a  $2^\circ \times 1^\circ$  (lon  $\times$  lat) grid and a  $2.5^\circ \times 2.5^\circ$  (lon  $\times$  lat) grid, respectively. The vertical wind shear is defined as the difference in zonal wind between 200 and 850 hPa, U200–U850. ASO seasonal mean SST and vertical wind shear are obtained by averaging together the three monthly mean values.

The CFS retrospective forecasts for 1981–2006 (Saha et al. 2006) are used in this study. The CFS is a fully coupled ocean–atmosphere–land model, which was implemented for operational climate forecasts at NCEP in 2004. The current version of the CFS has a horizontal resolution of T62, equivalent to nearly a 200-km Gaussian grid. This state-of-the-art dynamical forecast system has demonstrated skillful seasonal forecasts for a number of important climate phenomenons, including ENSO (Wang et al. 2005; Zhang et al. 2007), the African monsoon (Thiaw and Mo 2005), the Asian–Australian monsoon (Yang, et al. 2008; Wang et al. 2008), and the North American monsoon (Yang et al. 2008). A detailed description of model physics, hindcast configuration, and an overview of CFS performance can be found in Saha et al. (2006).

The 26-yr CFS hindcast data set is used to establish the statistical relationship between the observed Atlantic seasonal hurricane activity and the CFS predicted

variability of the atmosphere and oceans for ASO. *This procedure is different from the statistical methods that use preseason observations of the predictors for forecasting seasonal hurricane activity.*

The CFS hindcasts for the ASO season, with initial conditions (ICs) from April, May, June, and July, respectively, which correspond to 3, 2, 1, and 0-month lead forecasts, are used. For each initial month, the coupled model forecasts were run for nine months using 15 ICs. The ICs were clustered in three groups of five consecutive days centered on the 11th and 21st of the initial month, and the first day of the following month. For the atmosphere, the ICs were obtained from R2 and for the ocean from the NCEP Global Ocean Data Assimilation System (GODAS; Behringer and Xue 2004). The CFS ASO season hindcasts are based on an ensemble of the 15 members.

The CFS predictive skill for ASO SSTs and vertical wind shear is cross-validated by correlating CFS forecasts with the observations. The forecast anomaly of an ASO season is defined as the deviation from a 25-yr seasonal mean climatology that does not include the target season. The statistical significance of the correlations is estimated by the Monte Carlo technique (e.g., Wilks 1995). In addition, the CFS predictive skill is also compared with persisted anomaly forecasts, in which the observed SST and vertical wind shear anomalies at the initial time are persisted throughout the forecast period.

With the CFS predicted SSTs and vertical wind shear as predictors, the empirical prediction system requires three steps to make a target year forecast for Atlantic seasonal hurricane activity. The first step is to perform a simple linear (one predictor only) or multiple linear (multiple predictors) regression analysis between the area-averaged CFS hindcast SST/vertical wind shear anomalies in ASO and the observed interannual

variation of the Atlantic hurricanes over the 26-yr hindcast period. As stated above, the target year is removed from the regression analysis. The regression coefficients are then applied to the appropriate predictors from the CFS forecast for the target year to obtain the forecast of the interannual component of hurricane activity. Finally, the predicted interannual component obtained from the regression equation plus the long-term mean of the seasonal hurricane activity defines the total number of hurricanes for the target year.

There are two ways to define the long-term climatology of the seasonal hurricane activity. The first method (Method 1) uses the average of the Atlantic seasonal hurricanes over the entire 26 years (1981–2006), and gives a climatology of 6.2 hurricanes. We will show in section 4 that the upward hurricane trend (Fig. 1) cannot be inferred from the predictors derived from the CFS hindcasts, but closely ties to the observed preseason North Atlantic SSTs. Therefore, under the 26-yr mean climatology, the observed preseason North Atlantic SSTs are also employed as an additional predictor to represent the long-term variability of the hurricanes.

As shown in Fig. 1, the 26-yr Atlantic hurricane activity is characterized by an inactive period from 1981 to 1994 and an active period from 1995 to 2006. The second method for defining climatology (Method 2) is the use of a step function to represent the change in the climatological hurricane activity. Two mean states are obtained by averaging the seasonal hurricanes respectively over the inactive and active periods which gives a climatology of 4.6 hurricanes for the 1981–1994 period and 8.2 hurricanes for the 1995–2006 period. When using the step-function climatology, the predicted interannual change of the hurricane activity is added to the appropriate mean state to give the forecast of the total seasonal hurricanes.

The proposed empirical model differs from existing statistical forecast models in several ways. First, the predictors used in this model are derived from the CFS forecasts for the ASO season. In other words, dynamical forecasts provide the predictors used in the statistical model for predicting seasonal hurricane activity (e.g., Glahn and Lowry 1972). Second, the empirical forecast system utilizes the simultaneous relationship between the observed seasonal hurricane activity and the CFS predicted ASO SSTs and vertical wind shear. The statistical relationships in the empirical prediction model, therefore, reflect a link between the observed hurricane activity and the variability of model atmosphere and oceans. The proposed forecast method is thus a hybrid between statistical model and dynamical forecasts to predict the seasonal hurricane activity.

### **3. CFS predictive skill for SSTs and vertical wind shear**

The relationship between SSTs/vertical wind shear and Atlantic hurricane activity is the foundation for the seasonal hurricane prediction; therefore, we start with the analysis of the CFS predictive skill for these variables. Figure 2 (left panel) shows the spatial distribution of the anomaly correlation between observed and CFS predicted ensemble mean ASO SSTs from 3 to 0-month leads. Overall, CFS has significant skill in forecasting ASO SSTs in the eastern and central tropical Pacific, the ENSO-related SST region, and the tropical North Atlantic. As expected, the predictive skill is higher with shorter lead times. In both the tropical Pacific and MDR, the maximum correlations are above 0.6 at the 3-month lead (Fig. 2a) and above 0.9 at the 0-month lead (Fig. 2d).

The spatial maps of the anomaly correlation between observations and persisted anomaly forecasts are also shown in Fig. 2 (right panel). The persisted anomaly forecasts are the observed SST anomalies at the initial months of April, May, June, and July,

respectively, which are persisted throughout the ASO season. The CFS has a much higher forecast skill for the ASO SSTs than that based on persistence, especially at the 3-month to 1-month leads.

Figure 3 shows the spatial distribution of the anomaly correlation between the observed and CFS predicted vertical wind shear for ASO (left panel) and those with the persisted anomaly forecasts (right panel). Significant skill is found over the western tropical Pacific and equatorial Central/South America and adjacent oceans. The anomaly correlation is as high as 0.8 at the 3-month lead in both regions (Fig. 3a). While the skill continues to increase over the western Pacific with the decrease in forecast lead time, the skill shows little change over the west MDR. In the east MDR, the skill at the 3 and 2-month leads (Figs. 3a,b) is even slightly better than at the 1 and 0-month leads (Figs. 3c,d). As compared to SSTs in the MDR (Fig. 2), the predictive skill for vertical wind shear in the MDR is less sensitive to the length of the forecast lead time. Overall, the CFS (Figs 3a–3d) outperforms the persisted anomaly forecasts (Figs. 3e–3h) for the ASO vertical wind shear.

#### **4. Variability of Atlantic hurricanes and its relationship to SSTs and vertical wind shear**

We next analyze the observed seasonal hurricane variability and its relationship with the large-scale environmental factors, such as SSTs and vertical wind shear in the observations as well as in the CFS hindcasts. As shown in Fig. 1, Atlantic hurricanes exhibit substantial interannual variation and a strong upward trend, with an inactive period in the early years (1981–1994) and an active period in the recent years (1995–2006). Figure 4 shows the time series of the number of hurricanes from 1981 to 2006,

together with a linear trend, the step-function climatology, and the corresponding detrended and anomalous time series.

The upward trend indicates an increase of four hurricanes over the 26 years, equivalent to an increase of 1–2 hurricanes per decade. A 10-yr running mean time series of the Atlantic hurricanes from 1851 to 2006 (not shown), taken from the same hurricane dataset, suggests that the recent upward trend shown in Fig. 4a is a part of the multidecadal variation of the Atlantic hurricanes. This multidecadal variability is closely related to the AMO of SSTs (Enfield et al. 2001) through the Atlantic meridional mode (Kossin and Vimont 2007; Vimont and Kossin 2007).

The standard deviations of the total number of hurricanes (Fig. 4a) and detrended interannual component (Fig. 4b) are 3.0 and 2.6, respectively. The interannual variability contributes 75% to the total variance. This clearly indicates that the interannual change dominates the Atlantic hurricane variability. The standard deviation of the hurricane time series in Fig. 4c, which are the deviations from the step-function climatology, is 2.5. The interannual variations in the two time series in Figs. 4b and 4c, with different long-term changes taken out, are similar and highly correlated with a correlation of 0.94. The linear trend (Fig. 4a) and the detrended year-to-year fluctuations of the Atlantic hurricanes (Fig. 4b) are taken as two base time series used in the subsequent analysis.

To assess how the upward trend and interannual variability of Atlantic hurricanes are related to SSTs, Fig. 5 shows the correlation of ASO SSTs with the time series of the linear trend and interannual change in the seasonal hurricane activity, respectively. Correlations with the observations (Figs. 5a,d) and the CFS predictions (Figs. 5b,c,e,f) both reflect a relationship between the seasonal hurricane activity and SSTs in the ASO

season. The differences, therefore, depend on the SST predictive skill of the CFS for ASO as the target season with different lead times.

The correlation for the observed SSTs with the linear trend time series (Fig. 5a) is characterized by significant positive correlations in the North Atlantic with maximum values exceeding 0.7 in the MDR and to the north of 50°N. The spatial structure is similar to the North Atlantic multidecadal mode (Mestas-Nunez and Enfield 1999; Enfield et al. 2001; Bell and Chelliah 2006). The increase in Atlantic hurricane activity in the last two decades is thus associated with a warming of North Atlantic SSTs. Such a relationship has been well documented in many previous studies (e.g., Goldenberg et al. 2001; Bell and Chelliah 2006; Saunders and Lea 2008, among others), though the causes of this SST variability remain uncertain. We also note that strong correlations exist between the hurricane trend and pre-season North Atlantic SSTs (not shown). Over the Pacific, significant positive correlations are found in the tropical and extratropical western Pacific with no correlations in the equatorial eastern and central Pacific.

The CFS predicted SSTs for ASO exhibit some of these observed features (Figs. 5b,c), including significant positive correlations in the eastern North Atlantic between 20° and 40°N and at higher latitudes. The correlations with 3-month lead forecasts (Fig. 5b) are as strong as those for the 0-month lead (Fig. 5c). The largest discrepancy with the observations is a lack of strong correlation with the predicted SSTs in the MDR. In the Pacific sector, although significant positive correlations also exist in the extratropics, their location is shifted eastward. The results indicate that the CFS hindcast only partially reproduces the relationship between SSTs and the upward trend in the Atlantic hurricane activity.

On the interannual time scale, the correlations of CFS hindcast SSTs with Atlantic hurricanes (Figs. 5e,f) are similar to those for the observed SSTs (Figs. 5d) in the tropical Pacific. This is the canonical La Niña pattern with significant negative correlations in the eastern and central Pacific and positive correlations in the western Pacific. The ENSO influence on the Atlantic hurricanes, that is, a La Niña (El Niño) tends to increase (decrease) hurricane activity (Gray 1984a; Pielke and Landsea 1999; Elsner et al. 2001), is well preserved by the CFS hindcast SSTs due to the high skill of the CFS in predicting the ENSO SSTs (Wang et al. 2005; Zhang et al. 2007).

The strength of correlation with the CFS hindcast ASO SSTs depends on forecast lead time. The correlation with the 0-month lead forecast (Fig. 5f) is stronger in the tropical Pacific than that with the 3-month lead (Fig. 5e). The relatively low forecast skill for the tropical Pacific SSTs with the April IC (Fig. 5a) is primarily associated with the springtime predictability barrier (Saha et al. 2006). Similarly, in the MDR, the correlation for the 0-month lead (Fig. 5f) is stronger than for the 3-month lead (Fig. 5e), and further, is stronger than in the observations (Fig. 5d). We will show later in section 5 that the CFS predicted ASO SSTs with April and May ICs may not contribute to the Atlantic seasonal hurricane forecast. Finally, the correlations between anomalous SSTs with respect to their own step-function climatology for the 1981–1994 and 1995–2006 periods and the hurricane time series shown in Fig. 4c are very similar to those in Fig. 5 (not shown).

Based on the correlation analysis between the CFS hindcast SSTs and the observed interannual variability of Atlantic hurricanes, we choose SSTs averaged in the tropical Pacific (TPCF; 170°E–130°W, 5°S–5°N) and MDR as *two potential predictors*

for the interannual change in the hurricane activity. A close inspection of Figs. 2 and 5 reveals that the CFS predictive skill for ASO SSTs is also higher in those regions where SSTs primarily correlate with the hurricane interannual variability. The results provide confidence for using SSTs in the TPCF and MDR as the predictors for the interannual variability of the Atlantic hurricanes.

Shown in Fig. 6 are the correlations between vertical wind shear and the two base time series of the hurricane activity. The upswing in Atlantic hurricanes over the 26 years is strongly associated with decreased wind shear in the eastern MDR and equatorial eastern Atlantic (Fig. 6a). The distribution has a similar spatial structure to the wind shear anomaly that is related to the tropical multidecadal mode (Chelliah and Bell 2004; Bell and Chelliah 2006) and Atlantic meridional mode (Vimont and Kossin 2007).

The significant correlations in the eastern MDR and eastern tropical Atlantic shown in Fig. 6a are completely absent in the correlations with CFS hindcast wind shear (Figs. 6b,c). A small area of negative correlations at the northwest corner of the MDR in observations is found in the hindcasts with April (Fig. 6b) and May (not shown) ICs, but not with June (not shown) and July (Fig. 6c) ICs. Therefore, the CFS hindcast is not able to reproduce the observed wind shear trend (Fig. 1), which in the observations relates well with the recent increase in Atlantic hurricane activity (Goldenberg et al. 2001; Latif et al. 2007). Considering the importance of the wind shear trend and the limitation of CFS in predicting this trend, a practical alternative for a statistical prediction scheme is to use pre-season North Atlantic SSTs from observations as an additional predictor, which highly correlates with the hurricane trend and is expected to better represent the long-term change in the hurricane activity.

Associated with the interannual variability of the Atlantic hurricanes, significant negative correlations with vertical wind shear are found over Central America, equatorial South America, the Caribbean and eastern Pacific (Fig. 6d). The wind shear pattern resembles the negative of the composite wind shear anomaly based on the ENSO mode (Bell and Chelliah 2006). Indeed, vertical wind shear anomalies averaged over these regions (not shown) had a very strong wind shear in the 1982, 1987 and 1997 El Niño years not manifested in the wind shear anomalies averaged over the MDR (Fig. 1).

In contrast to the wind shear in the eastern MDR that is related to the upward hurricane trend (Fig. 6a), on the interannual time scale an active hurricane season tends to be associated with a decrease in vertical wind shear in the western MDR. The latter is also captured in the CFS hindcast at the 3-month lead (Fig. 6e). As the lead time decreases, the region of significant negative correlations extends to the eastern MDR (Fig. 6f). Note that the CFS predictive skill in the west MDR, where wind shear correlates more with the hurricane interannual variation, is also higher than in the east MDR (Fig. 3). The high correlations in the east MDR (Fig. 6f), not found in observations, are primarily due to a strong atmospheric response in the CFS to the tropical Pacific SSTs. The latter can significantly affect the interannual variability of the Atlantic hurricanes. The correlations between the vertical wind shear and the seasonal hurricane activity, after removing their corresponding step-function climatology (not shown), are very similar to Fig. 6 (right panel). Because the seasonal hurricane prediction is based on the relationship between the hurricane interannual variation and CFS predicted vertical wind shear (Figs. 6e,f), we choose vertical wind shear averaged in the MDR as *the third potential predictor* from the CFS seasonal forecasts.

The CFS forecast skill for the three predictors, i.e., ASO SSTs in the TPCF and MDR and vertical wind shear in the MDR is further examined. Shown in Fig. 7 are the 26-yr (1981–2006) time series of ASO seasonal mean SSTs averaged in the TPCF and MDR, the vertical wind shear in the MDR for both observations and CFS ensemble hindcasts, and the observed preseason SSTs averaged in the North Atlantic (NATL; 30°W–60°W, 55°N–65°N). The CFS hindcast SSTs are generally 1–2 K colder than observations in the TPCF (Fig. 7a), but slightly warmer ( $< 0.5$  K) in the MDR prior to 2002 (Fig. 7b) and cooler afterwards. The hindcast vertical wind shear is much weaker than observations in the MDR throughout the 26 years (Fig. 7c), especially at 3 and 2-month forecast leads. The corresponding linear trends in the CFS hindcasts are weaker than in the observations, especially for the MDR SST and vertical wind shear (Figs. 7b,c). These errors in the CFS SST and wind shear trend may be related to the use of fixed greenhouse gas concentration at the 1988 level in this version of the CFS and associated model drafts though the initial state for the CFS forecasts comes from observations (Cai et al. 2009).

In spite of these mean biases and weak trends, the CFS has good skill in predicting the interannual variability of SSTs and vertical wind shear in the TPCF and MDR. The correlation coefficients between the CFS hindcasts and observations are listed on the right side of Figs. 7a–7c using both original and detrended time series. For the TPCF SST (Fig. 7a), the correlation is 0.74 for the April ICs and increases to 0.94 for the July ICs. The 1982, 1987 and 1997 El Niño are well identified in Fig. 7a. The correlation for the detrended time series is slightly higher for the April–June ICs because the unrealistic downward trends in the CFS hindcasts are removed. The trend in the

hindcast SSTs with the July ICs is very close to the observed. Therefore, removing the two trends does not change the correlation (0.94). The forecasts for the interannual variability of TPCF SST (detrended) are highly skillful with a score of 0.9 or higher at 2-month and shorter leads.

The CFS forecasts for the MDR SST (Fig. 7b) are slightly less skillful when compared to the TPCF SST. However, as the lead time decreases from three to zero months, the skill for the interannual variability of the MDR SST (detrended) is significantly improved with an increase in the correlation from 0.57 to 0.93.

Unlike the predictive skill for SSTs, the skill for the MDR wind shear shows a minimum at the 1-month lead. The largest correlations (0.73) occur at the 2-month lead in the original time series and at the 0-month lead in the detrended time series. The non-monotonic feature of the forecast skill with lead time for vertical wind shear is also reflected in the spatial map of the anomaly correlations in the MDR (Fig. 3).

The preseason NATL SSTs (Fig. 7d) are dominated by a strong warming trend, with the interannual variability contributing less than 50% to the total variance. The correlations between the NATL SST and both the Atlantic seasonal hurricane activity and the hurricane trend are listed on the right side of Fig. 7d. The much higher correlations for the hurricane trend versus the storm count are consistent with the strong association between the AMO and the long-term variability of the Atlantic hurricanes. The January–February–March (JFM), February–March–April (FMA), March–April–May (MAM), and April–May–June (AMJ) seasonal mean NATL SSTs, together with the predictors from the CFS seasonal forecasts for ASO with April, May, June and July ICs, respectively, are used for developing the prediction system for the Atlantic seasonal hurricane activity.

We next examine the correlations between the three predictors from the CFS hindcasts and the hurricane trend and detrended time series (Figs. 4a,c). These correlations are listed in Table 1a. Consistent with the spatial distribution of the correlations in Fig. 5, the TPCF SST is significantly correlated with the interannual variability of hurricane activity, whereas the MDR SST is correlated more with the hurricane trend, except at the 0-month lead. The CFS predicted MDR wind shear displays strong correlations with the hurricane interannual variability at almost all lead times, also consistent with the corresponding correlation maps (Fig. 6).

Table 1b presents a correlation matrix for the detrended time series of the three predictors at different lead times and also their correlations with the interannual variability of the Atlantic hurricanes. Weak correlations between SSTs in the TPCF and MDR indicate that the interannual variations of SSTs in the two regions are largely independent. However, both predictors are significantly correlated with the MDR wind shear. The remote and local SSTs may exert their influences on the hurricane activity by altering the vertical wind shear over the MDR. The linkage between the TPCF SST and MDR wind shear in the CFS is stronger than that in the observations at all forecast lead times, whereas the linkage between the MDR SST and wind shear is comparable to the observations only at 1 and 0-month leads.

As the analysis so far is based on the ensemble mean of the CFS predictions, a procedure that enhances the common signal among predictions from different initial conditions, we also analyze the forecast skill and correlations using individual CFS predictions. Figure 8 presents the forecast skill for the three predictors for all 15 individual CFS runs. In general, the correlation between the ensemble mean forecast and

the observations is much higher than that of individual members, particularly for the vertical wind shear in the MDR (Figs. 8c,f). For the interannual variability of vertical wind shear (Fig. 8f), for example, no members have correlations higher than the ensemble mean forecast at 3 and 1-month leads. At 2 and 0-month leads, only one member shows a higher correlation than the ensemble mean. For the TPCF and MDR SSTs (Figs. 8a,b,d,e) at all lead times, no more than four members out of 15 produce better forecasts than the ensemble. The averages of correlations between the three predictors based on individual CFS members and the hurricane variability are also listed in Table 1a. These correlations are generally weaker than those with the ensemble mean CFS forecasts, especially for the interannual variability of the vertical wind shear. It is therefore expected that the predictors derived from the ensemble of forecasts are more effective than those from the individual CFS members for the seasonal hurricane forecast.

The spread of the forecast skill among the 15 members is evaluated by calculating the inter-member standard deviation of the correlations shown in Fig. 8. Overall, the forecasts for the TPCF SST have the smallest spread with the standard deviation ranging from 0.02 to 0.06, then the MDR SST with spread from 0.03 to 0.12, and finally the MDR wind shear with the largest spreads from 0.07 to 0.14. Except for the 2-month lead forecast for the TPCF SST, the spread becomes smaller as the lead time decreases. As seen in Fig. 8, the forecast uncertainty is significantly reduced at 1 and 0-month leads.

To summarize, the correlation analysis presented in Figs. 5 and 6 well separates the association of the seasonal hurricane activity with the ASO SSTs and vertical wind shear in terms of the trend and interannual variability. For both SSTs and wind shear, and for observations and CFS hindcasts, a region with a strong correlation with the

hurricane upward trend is generally less correlated with the hurricane interannual variability, and vice versa. The distinctions suggest that different physical processes are responsible for the two types of variability in the seasonal hurricane activity, which is also the basis for choosing specific regions to construct predictors. In general, the correlation between the hurricane interannual variability and the CFS hindcast wind shear is stronger than the correlation with the hindcast SSTs (Table 1). The vertical wind shear from CFS may have more predictive value than the SSTs.

## **5. Empirical prediction of seasonal hurricane activity with CFS**

Based on the analysis described in sections 3 and 4, the CFS predicted SSTs in the TPCF and MDR, vertical wind shear in the MDR for the ASO season, and observed preseason NATL SSTs are selected as potential predictors for seasonal hurricane activity. For Method 1, the number of Atlantic hurricanes is predicted based on multiple linear regression of the NATL SST and selected CFS predictors against the seasonal hurricane activity. When the step-function climatology (Fig. 4a) is used to represent the 1981–1994 inactive period and 1995–2006 active period, only the predictors from the CFS seasonal forecasts are used (Method 2). The skill of the forecasts for both methods is assessed by a cross-validation technique using the 26-yr CFS hindcasts. The forecast skill is quantified by the temporal correlation between the observed and forecasted seasonal hurricanes and also compared with the forecast skill using the same predictors but derived from persisted anomaly forecasts of SSTs and wind shear. The forecast skill assessed using the rank correlation (not shown) is qualitatively consistent with skill using the Pearson correlation.

Figure 9 (left panel) shows the hindcasts of the Atlantic hurricanes for the 1981–2006 seasons based on two SST predictors from the CFS, i.e., the TPCF SST and the MDR SST, together with the NATL SST from observations (Method 1). The hindcasts with the TPCF SST from the CFS capture the three inactive hurricane seasons of 1982, 1987 and 1997 (El Niño years), but miss the two active seasons of 1995 (La Niña year) and 2005 (Fig. 9a). In contrast, the hindcasts with the MDR SST capture the two active seasons of 1995 and 2005 at 1 and 0-month leads, but miss the three inactive seasons (Fig. 9b). Using both the remote and local SSTs as predictors gives better forecasts (Fig. 9c). The improvements are observed not only in the extreme years but also in some normal years, such as 2003 when the hindcast using each individual predictor (Figs. 9a,b) overestimates the number of hurricanes.

When using the observed pre-season NATL SST predictor, the forecast skill for the TPCF SST as the only CFS predictor is close to the skill using both the TPCF and MDR SST predictors at 3 to 1-month leads (Fig. 9d). The skill with the two predictors is considerably increased at the 0-month lead. The forecasts with only the MDR SST have virtually no skill at 3 and 2-month leads, but are more skillful than the TPCF SST at 0-month lead.

The skill for the hurricane hindcasts using the TPCF SST and MDR SST from persisted anomaly SST forecasts is shown in Fig. 9e. Except for those with the MDR SST at the 3 and 2-month leads, the hurricane hindcasts based on the CFS predicted SSTs are better than those based on the persisted SST anomalies (Fig. 9d vs. 9e).

Hindcasts for the 26-yr hurricane seasons are also made using the TPCF SST and MDR SST from the CFS as the only predictors under the step-function climatology for

the Atlantic hurricanes (Method 2). In this case, the number of hurricanes is the sum of the predicted interannual component and the average of the seasonal hurricanes over the 1981–1994 or 1995–2006 periods. The corresponding forecast skills are shown in Fig. 9f. At all lead times and using either one or both SST predictors, the hindcasts with the assumption of the step-function climatology are more skillful than those using the observed NATL SSTs as an extra predictor.

The hindcasts of the seasonal hurricane activity using the MDR vertical wind shear as the third predictor from the CFS are shown in Fig. 10. Incorporating the vertical wind shear into the seasonal hurricane forecast greatly improves the skill at all lead times. Particularly, in conjunction with the NATL SST (Method 1), the hindcasts using the MDR wind shear as the only predictor from the CFS are most skillful (Figs. 10a,d). Adding the TPCF SST (Fig. 10b,d) or both TPCF and MDR SSTs (Figs. 10c,d) does not increase the skill score. A possible explanation for this is that the vertical wind shear from the CFS seasonal forecast already contains the atmospheric response to SST forcing, meaning it already incorporates both the TPCF and MDR SSTs. This is indicated by the strong correlation between the MDR wind shear and both the TPCF and MDR SSTs (Table 1b), though the latter two are less correlated.

When using the persisted SST and wind shear anomalies as the predictors, the forecast skills (Fig. 10e) are comparable to those using the predictors from the CFS hindcasts (Fig. 10d) only at the 0-month lead. The hindcasts with the step function as the hurricane climatology (Fig. 10f; Method 2) are better than those with the NATL SST as an extra predictor (Fig. 10d; Method 1). The inclusion of the MDR wind shear also

improves the hindcasts based on the SSTs only and with the same step-function climatology (Figs. 9f vs. 10f).

To summarize, using either the observed preseason NATL SSTs (Method 1) or the step-function hurricane climatology (Method 2), for the seasonal hurricane forecast with CFS predicted SSTs, the TPCF SST is more skillful in inactive hurricane seasons whereas the MDR SST is more skillful in active seasons. The TPCF SST, however, has more predictive value than the MDR SST as indicated by the higher skill score. The combination of SSTs in both remote and local areas results in a better seasonal hurricane forecast. Given that the CFS is more skillful in predicting TPCF SST and MDR SST (Fig. 8), it is interesting to note that the MDR vertical wind shear from the CFS has the highest skill in predicting the seasonal hurricane activity. This is consistent with the largest correlation between the hurricane activity and the CFS ensemble mean MDR wind shear (Table. 1). More interestingly, the seasonal hurricane forecast with the MDR wind shear as the only predictor from the CFS is better than any combination of the three predictors. *The MDR wind shear is thus selected as the only predictor from the CFS seasonal forecast in the final configuration of the empirical prediction model.*

The statistical forecast model developed in this study is analyzed further by comparing it to previous forecasts issued by CSU (Klotzbach and Gray 2007) and NOAA (NOAA 2007) for the past six years (2002–2007). For this comparison, the data used in the regression analysis consist of only years prior to the target year. To make a forecast for 2002, for example, we use CFS predicted ASO MDR vertical wind shear and observed preseason NATL SSTs over the 1981–2001 period to establish the relationship to the observed hurricane activity using the multiple linear regression (Method 1). The

forecasts are then made based on this relationship, the NATL SSTs during January–June 2002, and the CFS predicted wind shear for ASO of 2002. Similarly, with the step-function climatology (Method 2), we use the CFS predicted MDR wind shear for ASO from 1981–2001 in the simple linear regression. The step-function climatology is defined by the average of the seasonal hurricanes over the 1981–1994 and 1995–2001 periods.

Table 2 lists the forecasts of the Atlantic hurricanes for the 2002–2007 seasons with the CFS predicted ASO MDR wind shear at 3-month (April ICs) and 0-month (July ICs) leads and those issued by CSU (Klotzbach and Gray 2007) in late May and early August and by NOAA (NOAA 2007) in middle May and early August. The actual number of hurricanes occurring in each year and the root mean square errors (RMSEs) of the forecasts over the six years are also listed in Table 2. The forecasts based on the regression equations are rounded to the nearest integer to obtain the number of hurricanes. A comparison among these forecasts indicates that the RMSEs for the forecasts at approximately the same lead time are very close to each other. This result suggests that the seasonal hurricane forecast based on the CFS predicted large-scale wind field is competitive with the current statistical forecast models. It is also noted that for the 2002–2007 seasons, the forecasts with the step-function climatology (Method 2) have a relatively larger RMSE than those with the NATL SST (Method 1). This is likely due to the shorter period of time used to define the climatology for the active period.

The empirical forecast model was also tested for the 2008 Atlantic hurricane season using operational seasonal forecasts from the CFS. The MDR wind shear is derived from the ensemble forecast of 60 members for the ASO 2008. The number of

ensemble members is large enough to estimate the uncertainty in the forecast. The empirical relationship used for the 2008 season is based on the data over the past 27 years from 1981 to 2007. The model was also used to predict the number of tropical storms and major hurricanes by replacing the time series of the Atlantic hurricanes in the regression analysis with the time series of the observed named storms and major hurricanes. Table 3 summarizes the forecasts made in the middle of May and early August for the 2008 season, including the number of hurricanes, named storms and major hurricanes, as well as the forecast range, which is determined by taking one standard deviation of the inter-member spread among the 60 members. The forecasts with either the NATL SST (Method 1) or the step-function climatology (Method 2) both agree with the observations reasonably well.

## **6. Conclusions**

In this paper the development of a statistical forecast model for predicting the hurricane activity during the Atlantic hurricane season is summarized. A unique feature of the model is that the predictors are from a dynamical seasonal prediction system, i.e., the CFS at NCEP. The prediction model is built upon the empirical relationship between the interannual variability of the actual number of hurricanes during the Atlantic hurricane season and the variability of SSTs and vertical wind shear in the CFS hindcasts for the ASO season.

The statistical model demonstrates considerable skill in predicting the interannual variability of Atlantic hurricanes when using either the observed NATL SSTs related to the hurricane trend (Method 1) or a step-function climatology changing from a generally inactive period to a very active period (Method 2). Cross-validations of the forecasts

using different combinations of the three selected predictors from the CFS hindcasts quantify their relative importance and predictive value when forecasting the seasonal hurricane activity.

The forecasts based on the CFS predicted SSTs suggest that when the TPCF SST is used as the only predictor from the CFS, the forecast is more skillful in inactive hurricane seasons, especially during El Niño years, and less skillful in active seasons. This implies that the influence of El Niño on seasonal hurricane activity may be stronger than that of La Niña, probably due to the nonlinearity associated with El Niño vs. La Niña (e.g., Hoerling et al. 1997). In contrast, the MDR SST as the only predictor from the CFS is more skillful in active seasons and less skillful in inactive seasons. Local SSTs seem to contribute to increased hurricane activity at the interannual time scale similarly to how they contribute to the increases over the past decade (Goldenberg et al. 2001; Saunders and Lea 2008). Overall, the TPCF SST has more predictive value than the MDR SST for the interannual variability of hurricane activity. When both the TPCF SST and MDR SST are used as predictors, the remote and local SSTs may complement each other and give a better forecast.

The forecasts with the MDR vertical wind shear as the only predictor from the CFS are more skillful compared to those using SST predictors. Adding the remote and local SSTs as additional predictors to the model does not improve the forecast skill, because the influence and information from SST variability already exist in the CFS forecasted atmospheric circulation over the MDR during ASO. Therefore, a statistical model based on simultaneous relationships may not require as many predictors as a model based on lagged relationships.

There are some aspects that can be further improved in this model. For example, it has been shown that forecasting the number of hurricanes can be significantly improved using a Poisson regression (Elsner and Schemertmann 1993), which is a nonlinear regression analysis and is more appropriate to count data like the number of hurricanes. Another possible extension is the use of individual CFS predictions to develop a probabilistic hurricane forecasting system, where not only the central tendency for seasonal hurricane activity, but also the distribution around this tendency can also be specified.

*Acknowledgments.* This work was supported by the NOAA Climate Test Bed (CTB) Program. We thank Drs. Kingse C. Mo, David Unger, Jon Gottschalck and three anonymous reviewers for their insightful and constructive comments and suggestions.

## REFERENCES

- Alves, O., G. Wang, A. Zhong, N. Smith, G. Warren, A. Marshall, F. Tzeitkin, and A. Schiller, 2002: POAMA: Bureau of Meteorology operational coupled model season forecast system. *Proc. ECMWF Workshop on the Role of the Upper Ocean in Medium and Extended Range Forecasting*, Reading, United Kingdom, ECMWF, 22–32.
- Behringer, D. W., and Y. Xue, 2004: Evaluation of the global ocean data assimilation system at NCEP: The Pacific Ocean. *Eighth Symposium on Integrated Observing and Assimilation System for Atmosphere, Oceans and Land Surface*, AMS 84th Annual Meeting, Seattle, Washington, 11–15 January 2004.
- Bell, G. D., and M. Chelliah, 2006: Leading tropical modes associated with interannual and multidecadal fluctuations in North Atlantic hurricane activity. *J. Climate*, **19**, 590–612.

- Bengtsson, L., K. I. Hodges, and M. Esch, 2007: Tropical cyclones in a T159 resolution global climate model: comparison with observations and re-analyses. *Tellus*, **59A**, 396–416.
- Cai, M., C. Shin, H. M. van den Dool, W. Wang, S. Saha, and A. Kumar, 2009: The role of long-term trend in seasonal predictions: Implication of global warming in the NCEP CFS. *Weather and Forecasting*, submitted.
- Chelliah, M., and G. D. Bell, 2004: Tropical multidecadal and interannual climate variability in the NCEP–NCAR reanalysis. *J. Climate*, **17**, 1777–1803.
- Elsner, J. B., B. H. Bossak, and X. Niu, 2001: Secular changes to the ENSO–U.S. hurricanes relationship. *Geophys. Res. Lett.*, **28**, 4123–4126.
- Elsner, J. B., and C. P. Schmertmann, 1993: Improving extended-range seasonal predictions of intense Atlantic hurricane activity. *Wea. Forecast*, **8**, 345–351.
- Emanuel, K., 2005: Increasing destructiveness of tropical cyclones over the past 30 years. *Nature*, **436**, 686–688.
- Enfield, D. B., A. M. Mestas-Nuñez, and P. J. Trimble, 2001: The Atlantic multidecadal oscillation and its relation to rainfall and river flows in the continental U.S. *Geophys. Res. Lett.*, **28**, 2077–2080.
- Glahn, H. R., and D. A. Lowry, 1972: The use of model output statistics (MOS) in objective weather forecasting. *J. Appl. Meteor.*, **11**, 1203–1211.
- Goldenberg, S. B., C. W. Landsea, A. M. Mestas-Nuñez, and W. M. Gray, 2001: The recent increase in Atlantic hurricane activity: Cause and implications. *Science*, **293**, 474–479.
- Goldenberg, S. B., and L. J. Shapiro, 1996: Physical mechanisms for the association of El Niño and West African rainfall with Atlantic major hurricane activity. *J. Climate*, **9**, 1169–1187.
- Gray, W. M., 1984a: Atlantic seasonal hurricane frequency. Part I: El Niño and 30-mb quasi-biennial oscillation influences. *Mon. Wea. Rev.*, **112**, 1649–1668.

- Gray, W. M., 1984b: Atlantic seasonal hurricane frequency. Part II: Forecasting its variability. *Mon. Wea. Rev.*, **112**, 1669–1683.
- Hess, J. C., and J. B. Elsner, 1994: Historical developments leading to current forecast models of annual Atlantic hurricane activity. *Bull. Amer. Meteor. Soc.*, **75**, 1611–1621.
- Hoerling, M. P., A. Kumar, and M. Zhong, 1997: El Niño, La Niña, and the nonlinearity of their teleconnections. *J. Climate*, **10**, 1769–1786.
- Ji, M., A. Kumar, and A. Leetmaa, 1994: Development of seasonal climate forecast system using coupled ocean-atmosphere model at National Meteorological Center. *Bull. Amer. Meteor. Soc.*, **75**, 569–577.
- Kanamitsu, M., W. Ebisuzaki, J. Woollen, S.-K. Yang, J. J. Hnilo, M. Fiorino, and G. L. Potter, 2002: NCEP–DOE AMIP-II Reanalysis (R-2). *Bull. Amer. Meteor. Soc.*, **83**, 1631–1643.
- Kanamitsu, M., and Coauthors, 2002: NCEP dynamical seasonal forecast system 2000. *Bull. Amer. Meteor. Soc.*, **83**, 1019–1037.
- Klotzbach, P. J., 2007: Recent development in statistical prediction of seasonal Atlantic basin tropical cyclone activity. *Tellus*, **59A**, 511–518.
- Klotzbach, P. J., and W. M. Gray, 2007: Extended range forecast of Atlantic seasonal hurricane activity and U.S. landfall strike probability for 2008. [Available online at <http://hurricane.atmos.colostate.edu/>]
- Knutson, T. R., J. J. Sirutis, S. T. Garner, I. M. Held, and R. E. Tuleya, 2007: Simulation of the recent multidecadal increase of Atlantic hurricane activity using an 18-km-grid regional model. *Bull. Amer. Meteor. Soc.*, **88**, 1549–1565.
- Kossin, J. P., and D. J. Vimont, 2007: A more general framework for understanding Atlantic hurricane variability and trends. *Bull. Amer. Meteor. Soc.*, **88**, 1767–1781.
- Landsea, C. W., and Coauthors, 2004: The Atlantic hurricane database re-analysis project: Documentation for the 1851–1910 alterations and additions to the HURDAT

- database. Hurricanes and Typhoons: Past, Present and Future. R. J. Murname and K.-B. Liu, Eds., Columbia University Press, 177–221.
- Latif, M., N. Keenlyside, and J. Bader, 2007: Tropical sea surface temperature, vertical wind shear, and hurricane development. *Geophys. Res. Lett.*, **34**, L01710, doi:10.1029/2006GL027969.
- Mason, S. J., L. Goddard, N. E. Graham, E. Yulaeva, L. Sun, and P. A. Arkin, 1999: The IRI seasonal climate prediction system and the 1997/98 El Niño event. *Bull. Amer. Meteor. Soc.*, **80**, 1853–1873.
- Mestas-Nunez, A. M., and D. B. Enfield, 1999: Rotated global modes of non-ENSO sea surface temperature variability. *J. Climate*, **12**, 2734–2746.
- NOAA, 2007: Atlantic Hurricane Outlook and Summary Archive. [Available online at <http://www.cpc.ncep.noaa.gov/>]
- Palmer, T. N., and Coauthors, 2004: Development of a European multimodel ensemble system for seasonal-to-interannual prediction (DEMETER). *Bull. Amer. Meteor. Soc.*, **85**, 853–872.
- Pielke, Jr., R. A., and C. N. Landsea, 1999: La Niña, El Niño, and Atlantic hurricane damages in the United States. *Bull. Amer. Meteor. Soc.*, **80**, 2027–2033.
- Reynolds, R. W., N. A. Rayner, T. M. Smith, D. C. Stokes, and W. Wang, 2002: An improved in situ and satellite SST analysis for climate. *J. Climate*, **15**, 1609–1625.
- Saha, S., and Coauthors, 2006: The NCEP Climate Forecast System. *J. Climate*, **19**, 3483–3517.
- Saunders, M. A., and A. S. Lea, 2008: Large contribution of sea surface warming to recent increase in Atlantic hurricane activity. *Nature*, **451**, 557–560.
- Thiaw, W. M., and K. C. Mo, 2005: Impact of sea surface temperature and soil moisture on seasonal rainfall prediction over the Sahel. *J. Climate*, **18**, 5330–5343.
- Vimont, D. J., and J. P. Kossin, 2007: The Atlantic Meridional Mode and hurricane activity. *Geophys. Res. Lett.*, **34**, L07709, doi:10.1029/2007GL029683.

- Vitart, F., and Coauthors, 2007: Dynamically-based seasonal forecasts of Atlantic tropical storm activity issued in June by EUROSIP. *Geophys. Res. Lett.*, **34**, L16815, doi: 10.1029/2007GL030740.
- Vitart, F., and T. N. Stockdale, 2001: Seasonal forecasting of tropical storms using coupled GCM integrations. *Mon. Wea. Rev.*, **129**, 2521–2537.
- Wang, B., and Coauthors, 2008: How accurately do coupled climate models predict the leading modes of Asian-Australian monsoon interannual variability? *Climate Dyn.*, submitted.
- Wang, W., S. Saha, H.-L. Pan, S. Nadiga, and G. White, 2005: Simulation of ENSO in the new NCEP Coupled Forecast System Model (CFS03). *Mon. Wea. Rev.*, **133**, 1574–1593.
- Webster, P. J., G. J. Holland, J. A. Curry, and H.-R. Chang, 2005: Changes in tropical cyclone number, duration and intensity in a warming environment. *Science*, **309**, 1844–1846.
- Wilks, D. S., 1995: *Statistical Methods in the Atmospheric Sciences*. Academic Press, pp. 467.
- Yang, S., Z. Zhang, V. E. Kousky, R. W. Higgins, S.-H. Yoo, J. Liang, and Y. Fan, 2008: Simulations and seasonal prediction of the Asian summer monsoon in the NCEP Climate Forecast System. *J. Climate*, in press.
- Yang, S., Y. Jiang, D. Zheng, R. W. Higgins, Q. Zhang, V. E. Kousky, and M. Wen, 2008: Variability of regional precipitation and associated physical processes in the NCEP CFS: Focus on the Southwest United States. *J. Climate*, submitted.
- Zhang, Q., A. Kumar, Y. Xue, W. Wang, and F.-F. Jin, 2007: Analysis of the ENSO cycle in the NCEP Coupled Forecast Model. *J. Climate*, **20**, 1265–1284.
- Zehr, R. M., and J. A. Knaff, 2007: Atlantic major hurricanes, 1995–2005—Characteristics based on best-track, aircraft, and IR images. *J. Climate*, **20**, 5865–5888.

### Figure Captions:

Fig. 1. Observed time series of the number of hurricanes (thick solid) during the Atlantic hurricane season, ASO mean SST anomaly (thin solid line with open circle) and vertical wind shear anomaly (dash line with open square) averaged in the MDR from 1981 to 2006. The negative of vertical wind shear anomaly,  $-(U_{200}-U_{850})$ , is plotted so that it displays an in-phase relationship with the seasonal hurricane activity.

Fig. 2. Spatial distribution of anomaly correlation between observed and CFS predicted ASO SSTs (left panel) and between observed and persisted anomaly forecasts (right panel) over the period 1981–2006. The CFS predicted SSTs are 15-member ensemble forecasts with (a) April, (b) May, (c) June, and (d) July initial conditions (ICs). The persisted anomaly forecasts are the observed SST anomalies at the initial months of (e) April, (f) May, (g) June, and (h) July that are persisted throughout the forecast period. Correlations exceeding the 1% significance level, estimated by the Monte Carlo tests, are shaded. Contours are 0.6, 0.8, and 0.9 with different darker shadings. Boxes indicate the tropical Pacific (TPCF;  $170^{\circ}\text{E}-130^{\circ}\text{W}$ ,  $5^{\circ}\text{S}-5^{\circ}\text{N}$ ) and MDR ( $20^{\circ}\text{W}-80^{\circ}\text{W}$ ,  $10^{\circ}\text{N}-20^{\circ}\text{N}$ ) where SSTs are averaged and used as predictors for Atlantic seasonal hurricane forecast.

Fig. 3. Same as in Fig. 2 but for vertical wind shear ( $U_{200}-U_{850}$ ). Box indicates the Atlantic hurricane MDR where wind shear is averaged and used as a predictor for Atlantic seasonal hurricane forecast.

Fig. 4. (a) Time series of the number of hurricanes during the Atlantic hurricane season from 1981 to 2006, (b) same time series after removing a linear trend, which is indicated by a straight line in (a), and (c) same time series after removing a step-function climatology, which is indicated by a dot line in (a).

Fig. 5. Correlations of (a),(d) observed and (b),(c),(e),(f) CFS predicted ASO SSTs with the 26-yr (1981–2006) time series of Atlantic seasonal hurricane linear trend (left) and detrended interannual variation (right). The CFS predicted SSTs are 15-member ensemble forecasts with (b),(e) April and (c),(f) July initial conditions. Contour interval is 0.1, with negative values dashed. Contours between  $-0.3$  and  $0.3$  are omitted. Shadings indicate correlations above the 1% significance level, estimated by the Monte Carlo tests. Boxes are the same as in Fig. 2.

Fig. 6. Same as in Fig. 5 but for vertical wind shear. Boxes are the same as in Fig. 3.

Fig. 7. Time series (1981–2006) of ASO SSTs averaged in (a) TPCF and (b) MDR, and (c) vertical wind shear averaged in MDR from observations (thick solid) and CFS 15-member ensemble forecasts with April (thick dot), May (thin solid), June (dash), and July (thick solid grey) initial conditions, and (d) observed preseason SSTs averaged in NATL in JFM (thick doc), FMA (thin solid), MAM (dash) and AMJ (thick solid grey). Straight lines indicate linear trends of corresponding time series. Correlations between the time series of the observations and CFS forecasts for each initial condition and those of detrended time series are listed on the right side of (a,b,c). On the right side of (d) are the correlations between the preseason NATL SST and both the seasonal hurricane activity and hurricane trend.

Fig. 8. Correlations between observed and CFS predicted ASO SSTs averaged in the TPCF (top panels) and MDR (middle panels), and vertical wind shear in the MDR (bottom panels) for 15 individual runs (grey) and 15-member ensemble (black). Left panels are the correlations with original time series and right panels with detrended time series. On each set of bars, the first value is the number of individual runs that have

higher correlations than the ensemble mean forecast and the second value the inter-member standard deviation of the correlations.

Fig. 9. (a)–(c) Observations (thick solid) and hindcasts of Atlantic hurricanes based on observed preseason NATL SSTs (Method 1) and CFS predicted ASO SSTs with April (thick dot), May (thin solid), June (dash), and July (thick solid grey) initial conditions, and correlations between the observations and hindcasts of the seasonal hurricanes for (d) Method 1, (e) also Method 1 but SST predictors from persisted anomaly forecasts and (f) Method 2, respectively. The hurricane hindcasts are based on ASO (a) TPCF SST, (b) MDR SST, and (c) both TPCF SST and MDR SST as the predictors. Light grey, grey and black bars in (d)–(f) indicate the correlations between observations and forecasts when using the TPCF SST (light grey), the MDR SST (grey) or both SSTs (black) as the predictors, respectively. The dash and solid lines in (d,e,f) indicate the 5% and 1% significance levels estimated by the Monte Carlo tests.

Fig. 10. Same as in Fig. 9 but for hurricane hindcasts using CFS predicted ASO (a) MDR vertical wind shear, (b) MDR wind shear and TPCF SST, and (c) MDR wind shear, TPCF SST and MDR SST as the predictors. Light grey, grey and black bars in (d)–(f) indicate the correlations between observations and hindcasts when using the MDR wind shear (light grey), MDR wind shear and TPCF SST (grey) and MDR wind shear, TPCF and MDR SSTs (black), respectively, for (d) Method 1, (e) Method 1 with predictors from persisted anomaly forecasts and (f) Method 2.

Table 1. (a) Correlations of the three predictors with the hurricane trend and detrended time series, respectively, over the period 1981–2006. The three predictors are derived from both observations and CFS ensemble forecasts for the ASO season with April–July initial conditions (ICs). Values in parentheses are the averages of correlations with individual CFS runs. (b) Correlation matrix of the detrended time series of the three predictors from both observations and CFS ensemble forecasts and also their correlation with the detrended number of seasonal hurricanes.

(a)

Predictor	TPCF SST		MDR SST		MDR U200–U850	
	Trend	Detrended	Trend	Detrended	Trend	Detrended
OBS	0.14	–0.56	0.69	0.36	–0.60	–0.45
IC Apr	–0.13 (–0.12)	–0.48 (–0.45)	0.34 (0.28)	0.06 (0.05)	–0.39 (–0.25)	–0.47 (–0.31)
IC May	–0.08 (–0.08)	–0.58 (–0.55)	0.42 (0.37)	0.14 (0.12)	–0.43 (–0.31)	–0.60 (–0.43)
IC Jun	0.03 (0.03)	–0.56 (–0.54)	0.40 (0.37)	0.38 (0.35)	–0.16 (–0.12)	–0.70 (–0.53)
IC Jul	0.11 (0.11)	–0.54 (–0.53)	0.47 (0.45)	0.50 (0.48)	–0.12 (–0.11)	–0.74 (–0.65)

(b)

Predictor	TPCF SST	MDR SST	MDR U200–U850	Hurricane
TPCF SST				
OBS	1.00	–0.15	0.43	–0.57
IC Apr	1.00	0.25	0.73	–0.49
IC May	1.00	0.11	0.72	–0.58
IC Jun	1.00	–0.20	0.84	–0.56
IC Jul	1.00	–0.30	0.75	–0.55
MDR SST				
OBS	–0.15	1.00	–0.55	0.50
IC Apr	0.25	1.00	–0.17	0.06
IC May	0.11	1.00	–0.36	0.15
IC Jun	–0.20	1.00	–0.50	0.41
IC Jul	–0.30	1.00	–0.67	0.56
MDR U200–U850				
OBS	0.43	–0.55	1.00	–0.56
IC Apr	0.73	–0.17	1.00	–0.52
IC May	0.72	–0.36	1.00	–0.67
IC Jun	0.84	–0.50	1.00	–0.71
IC Jul	0.75	–0.67	1.00	–0.75
Hurricane				
OBS	–0.57	0.50	–0.56	1.00
IC Apr	–0.49	0.06	–0.52	1.00
IC May	–0.58	0.15	–0.67	1.00
IC Jun	–0.56	0.41	–0.71	1.00
IC Jul	–0.55	0.56	–0.75	1.00

Table 2. Forecasts of the Atlantic hurricanes using the CFS predicted MDR vertical wind shear for ASO with April and July initial conditions (ICs) and those issued in late May and early August by CSU and in middle May and early August by NOAA for the 2002–2007 hurricane seasons. The forecasts based on the MDR wind shear use either observed preseason NATL SST (Method 1) or the step-function hurricane climatology (Method 2). The forecasts for Method 2 are listed in parentheses. The actual number of hurricanes (OBS) and root mean square error (RMSE) of the forecasts over the six years are also listed.

Year	CFS		CSU		NOAA		OBS
	Apr IC	Jul IC	Late May	Early Aug	Mid May	Early Aug	
2002	5 (7)	4 (5)	6	4	6–8	4–6	4
2003	8 (9)	7 (7)	8	8	6–9	7–9	7
2004	8 (8)	7 (7)	8	7	6–8	6–8	9
2005	9 (9)	11 (10)	8	10	7–9	9–11	15
2006	9 (9)	9 (8)	9	7	8–10	7–9	5
2007	11 (11)	9 (9)	9	8	7–10	7–9	6
RMSE	3.7 (3.9)	2.7 (2.8)	3.7	2.5	3.8	2.7	

Table 3. Forecasts issued in middle May and early August for the 2008 hurricane season based on the CFS predicted MDR wind shear for ASO. The forecasts include the number of hurricanes, named storms, major hurricanes, and forecast ranges, which is determined by  $\pm$  one standard deviation of inter-member spreads.

Predictor	MDR U200–U850 and NATL SST (Method 1)		MDR U200–U850 (Method 2)		OBS
	Mid May	Early Aug	Mid May	Early Aug	
Hurricane FCST Range	7 5–9	9 7–10	8 7–10	9 8–10	8
Named Storm FCST Range	13 9–16	14 13–16	14 11–17	15 14–17	16
Major Hurricane FCST Range	3 2–4	4 3–5	4 3–5	4 4–5	5

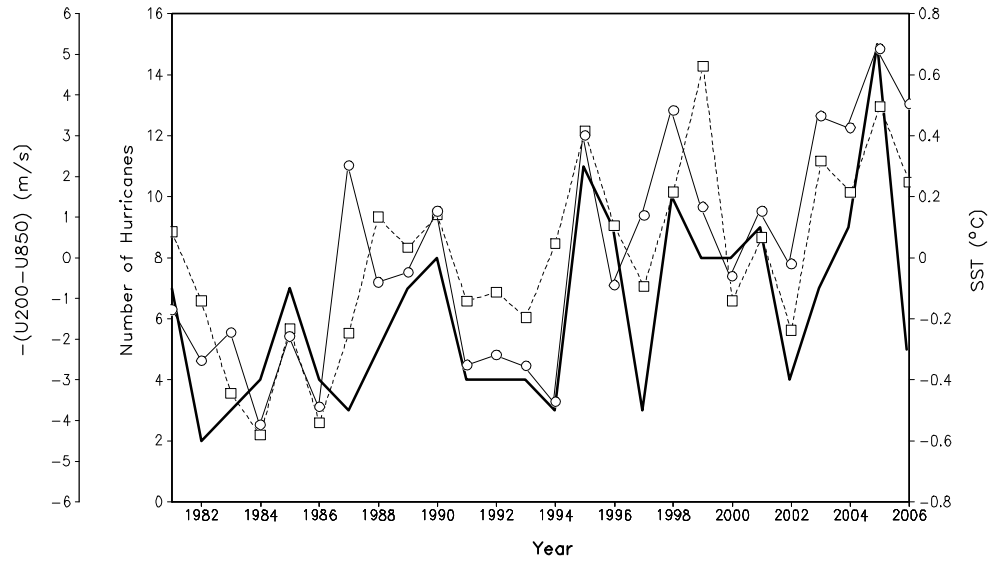


Fig. 1. Observed time series of the number of hurricanes (thick solid) during the Atlantic hurricane season, ASO mean SST anomaly (thin solid line with open circle) and vertical wind shear anomaly (dash line with open square) averaged in the MDR from 1981 to 2006. The negative of vertical wind shear anomaly,  $-(U_{200}-U_{850})$ , is plotted so that it displays an in-phase relationship with the seasonal hurricane activity.

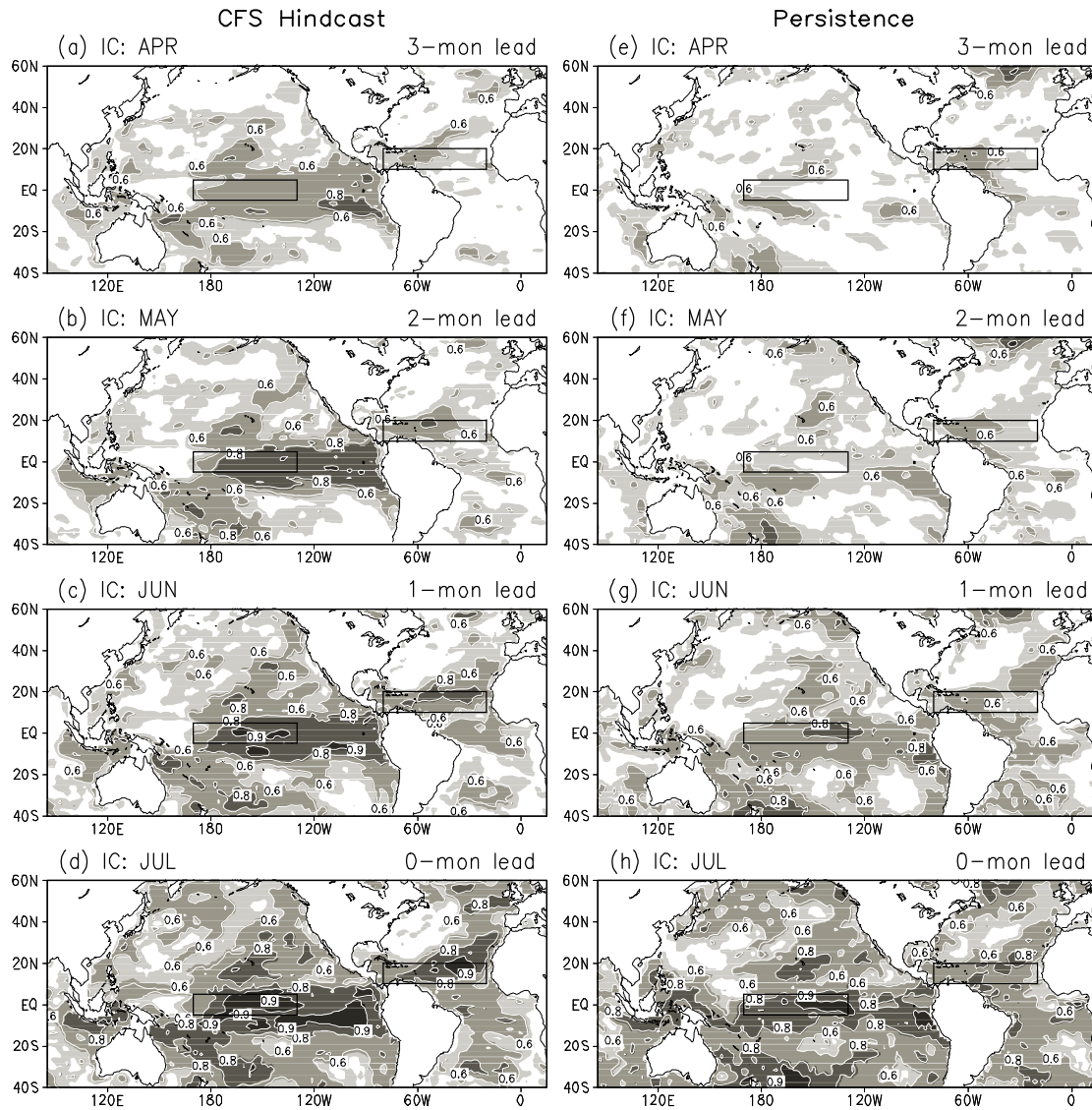


Fig. 2. Spatial distribution of anomaly correlation between observed and CFS predicted ASO SSTs (left panel) and between observed and persisted anomaly forecasts (right panel) over the period 1981–2006. The CFS predicted SSTs are 15-member ensemble forecasts with (a) April, (b) May, (c) June, and (d) July initial conditions (ICs). The persisted anomaly forecasts are the observed SST anomalies at the initial months of (e) April, (f) May, (g) June, and (h) July that are persisted throughout the forecast period. Correlations exceeding the 1% significance level, estimated by the Monte Carlo tests, are shaded. Contours are 0.6, 0.8, and 0.9 with different darker shadings. Boxes indicate the tropical Pacific (TPCF; 170°E–130°W, 5°S–5°N) and MDR (20°W–80°W, 10°N–20°N) where SSTs are averaged and used as predictors for Atlantic seasonal hurricane forecast.

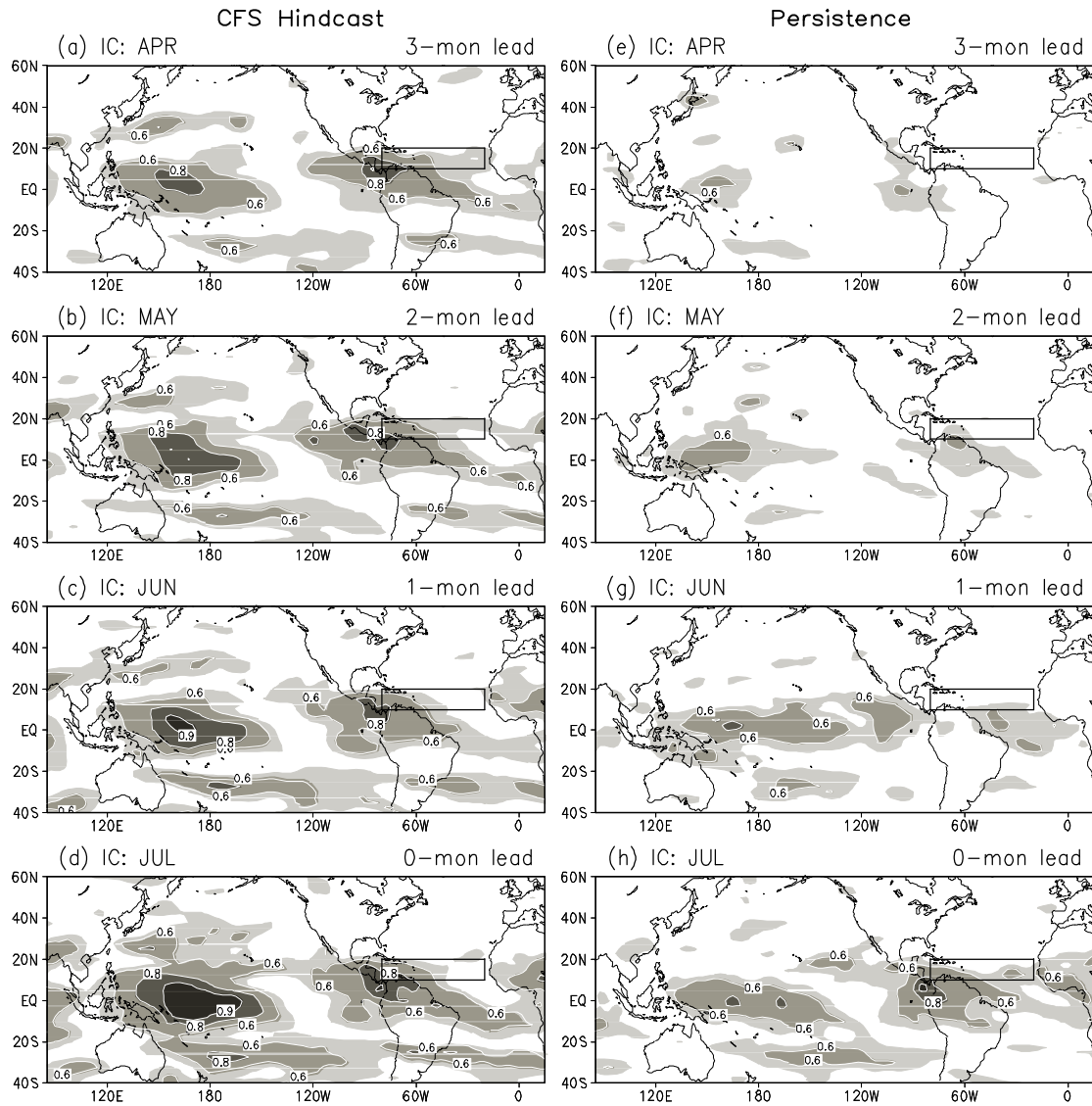


Fig. 3. Same as in Fig. 2 but for vertical wind shear ( $U_{200}-U_{850}$ ). Box indicates the Atlantic hurricane MDR where wind shear is averaged and used as a predictor for Atlantic seasonal hurricane forecast.

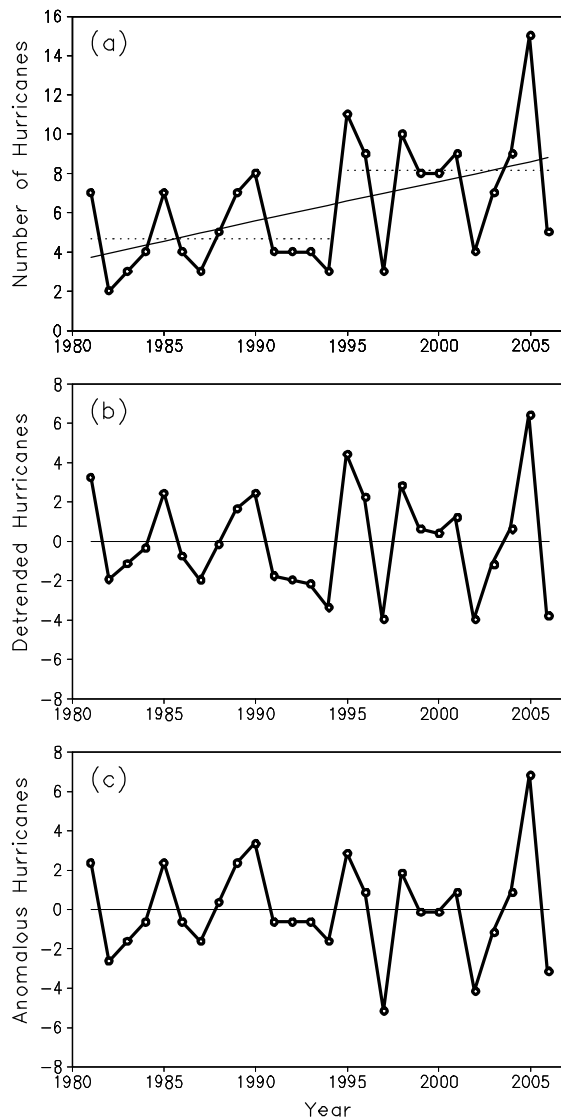


Fig. 4. (a) Time series of the number of hurricanes during the Atlantic hurricane season from 1981 to 2006, (b) same time series after removing a linear trend, which is indicated by a straight line in (a), and (c) same time series after removing a step-function climatology, which is indicated by a dot line in (a).

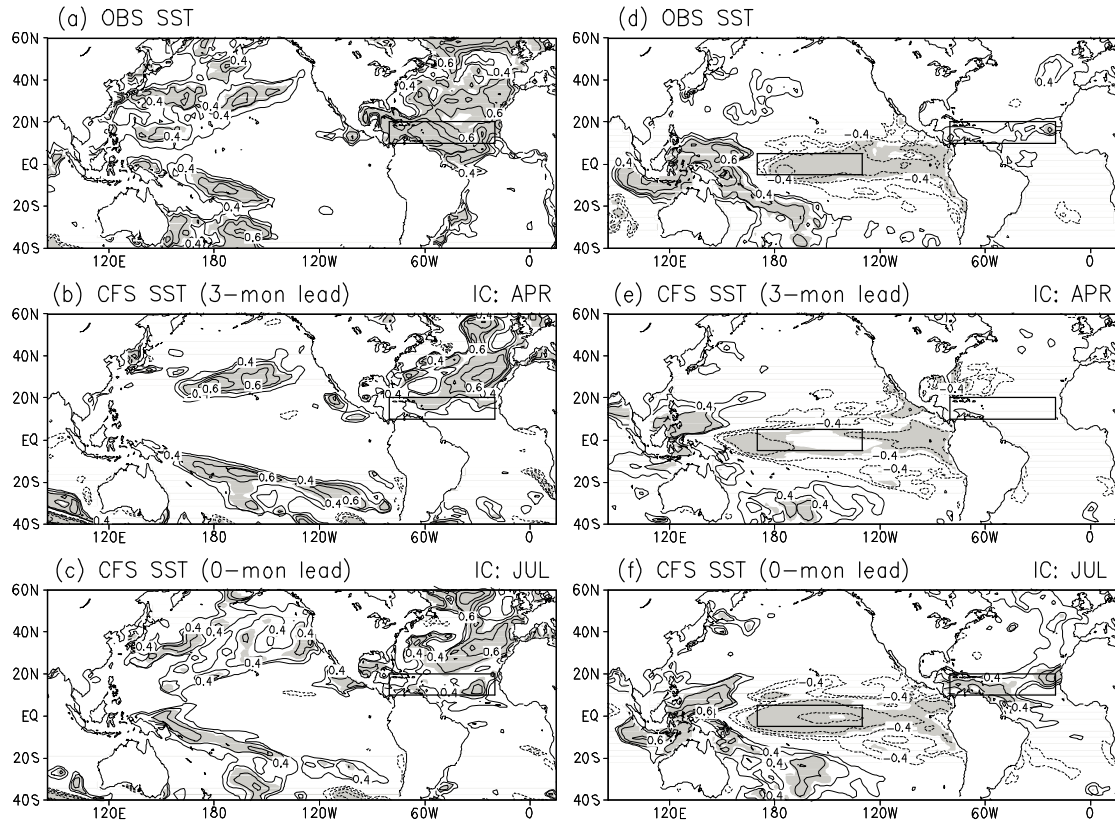


Fig. 5. Correlations of (a),(d) observed and (b),(c),(e),(f) CFS predicted ASO SSTs with the 26-yr (1981–2006) time series of Atlantic seasonal hurricane linear trend (left) and detrended interannual variation (right). The CFS predicted SSTs are 15-member ensemble forecasts with (b),(e) April and (c),(f) July initial conditions. Contour interval is 0.1, with negative values dashed. Contours between  $-0.3$  and  $0.3$  are omitted. Shadings indicate correlations above the 1% significance level, estimated by the Monte Carlo tests. Boxes are the same as in Fig. 2.

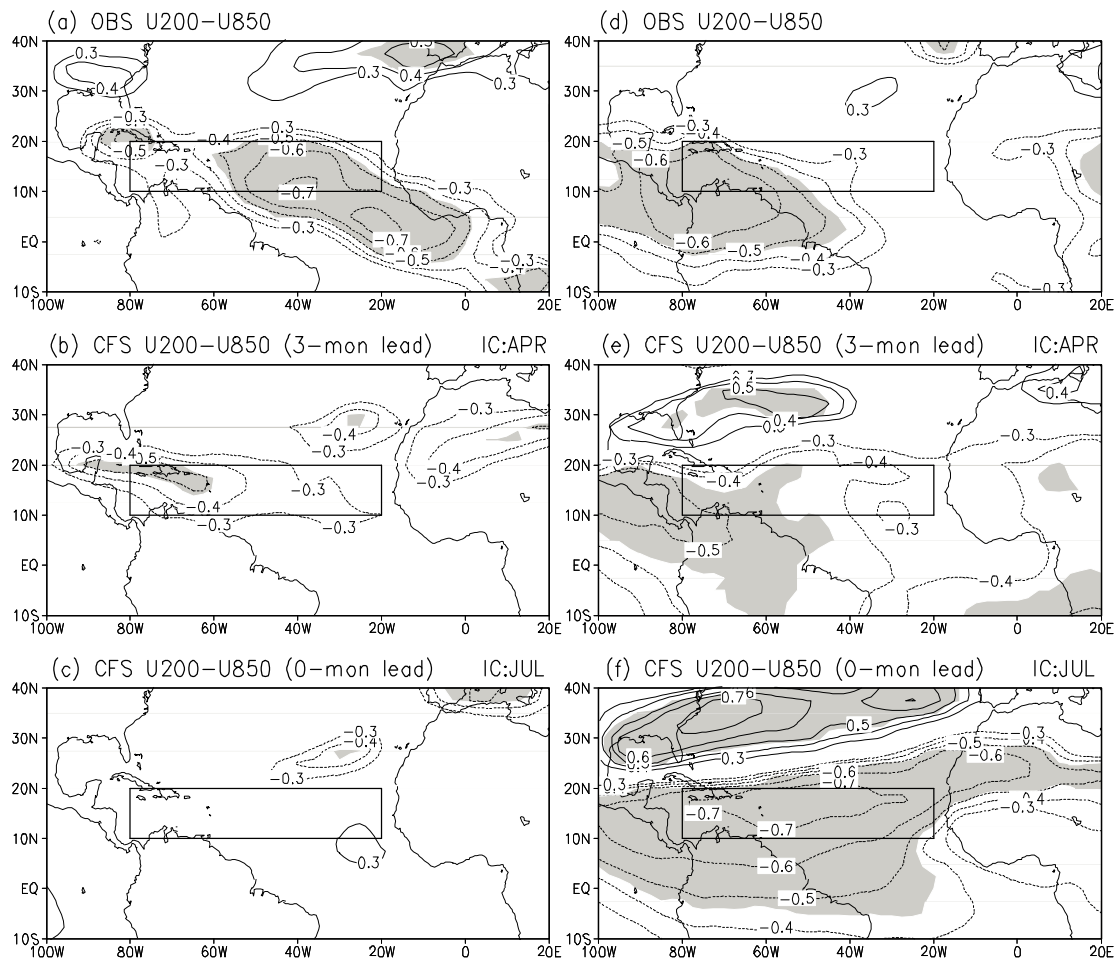


Fig. 6. Same as in Fig. 5 but for vertical wind shear. Boxes are the same as in Fig. 3.

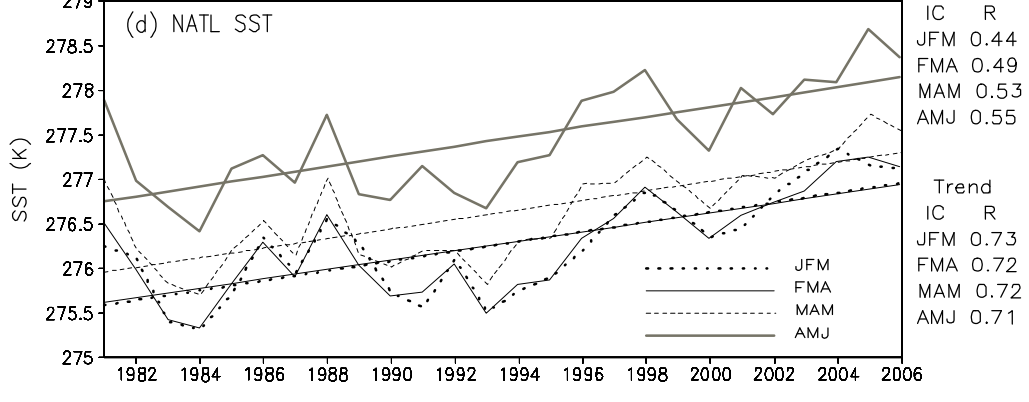
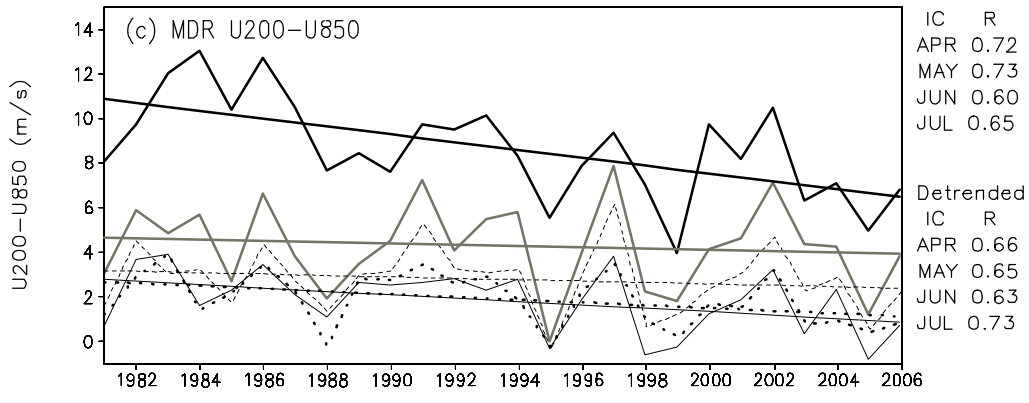
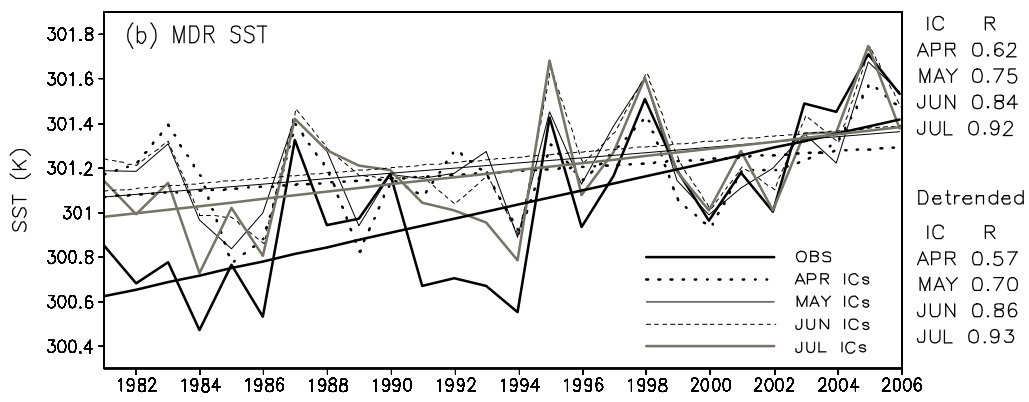
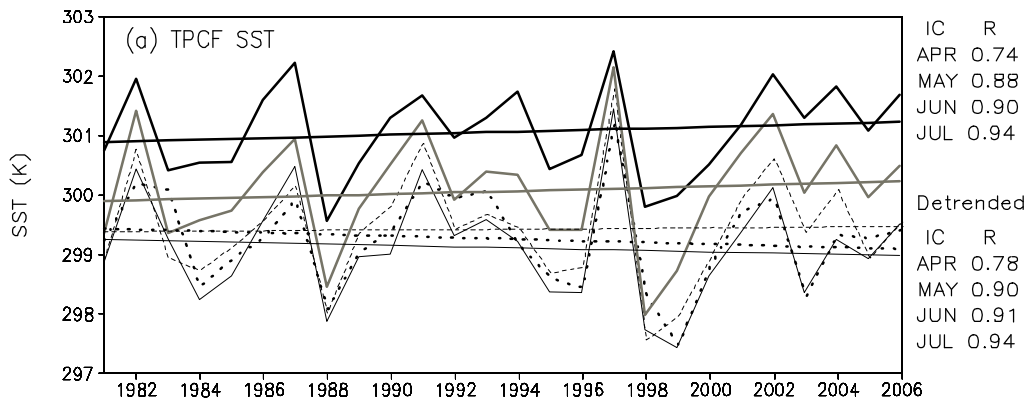


Fig. 7. Time series (1981–2006) of ASO SSTs averaged in (a) TPCF and (b) MDR, and (c) vertical wind shear averaged in MDR from observations (thick solid) and CFS 15-member ensemble forecasts with April (thick dot), May (thin solid), June (dash), and July (thick solid grey) initial conditions, and (d) observed pre-season SSTs averaged in NATL in JFM (thick dot), FMA (thin solid), MAM (dash) and AMJ (thick solid grey). Straight lines indicate linear trends of corresponding time series. Correlations between the time series of the observations and CFS forecasts for each initial condition and those of detrended time series are listed on the right side of (a,b,c). On the right side of (d) are the correlations between the pre-season NATL SST and both the seasonal hurricane activity and hurricane trend.

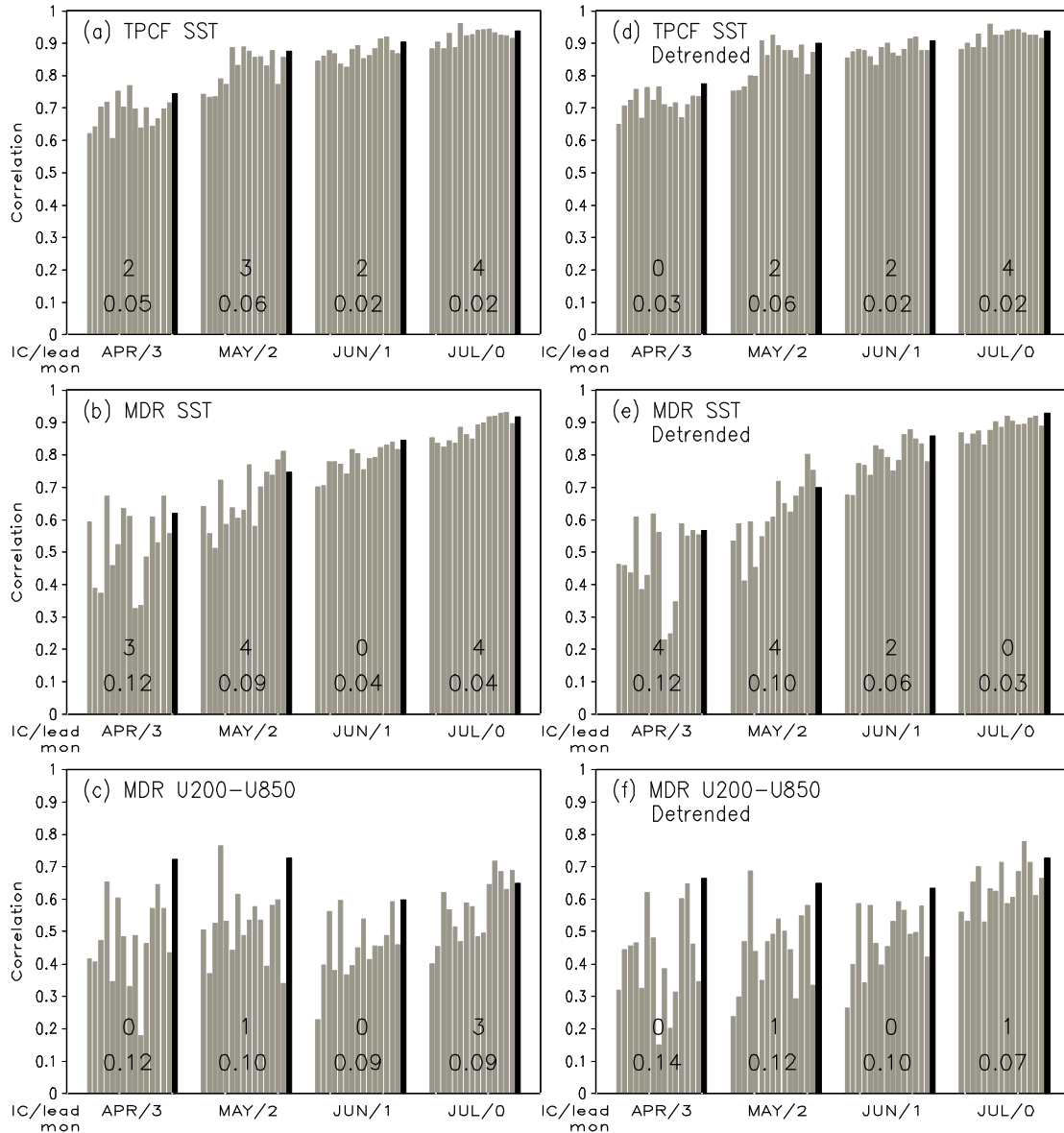


Fig. 8. Correlations between observed and CFS predicted ASO SSTs averaged in the TPCF (top panels) and MDR (middle panels), and vertical wind shear in the MDR (bottom panels) for 15 individual runs (grey) and 15-member ensemble (black). Left panels are the correlations with original time series and right panels with detrended time series. On each set of bars, the first value is the number of individual runs that have higher correlations than the ensemble mean forecast and the second value the inter-member standard deviation of the correlations.

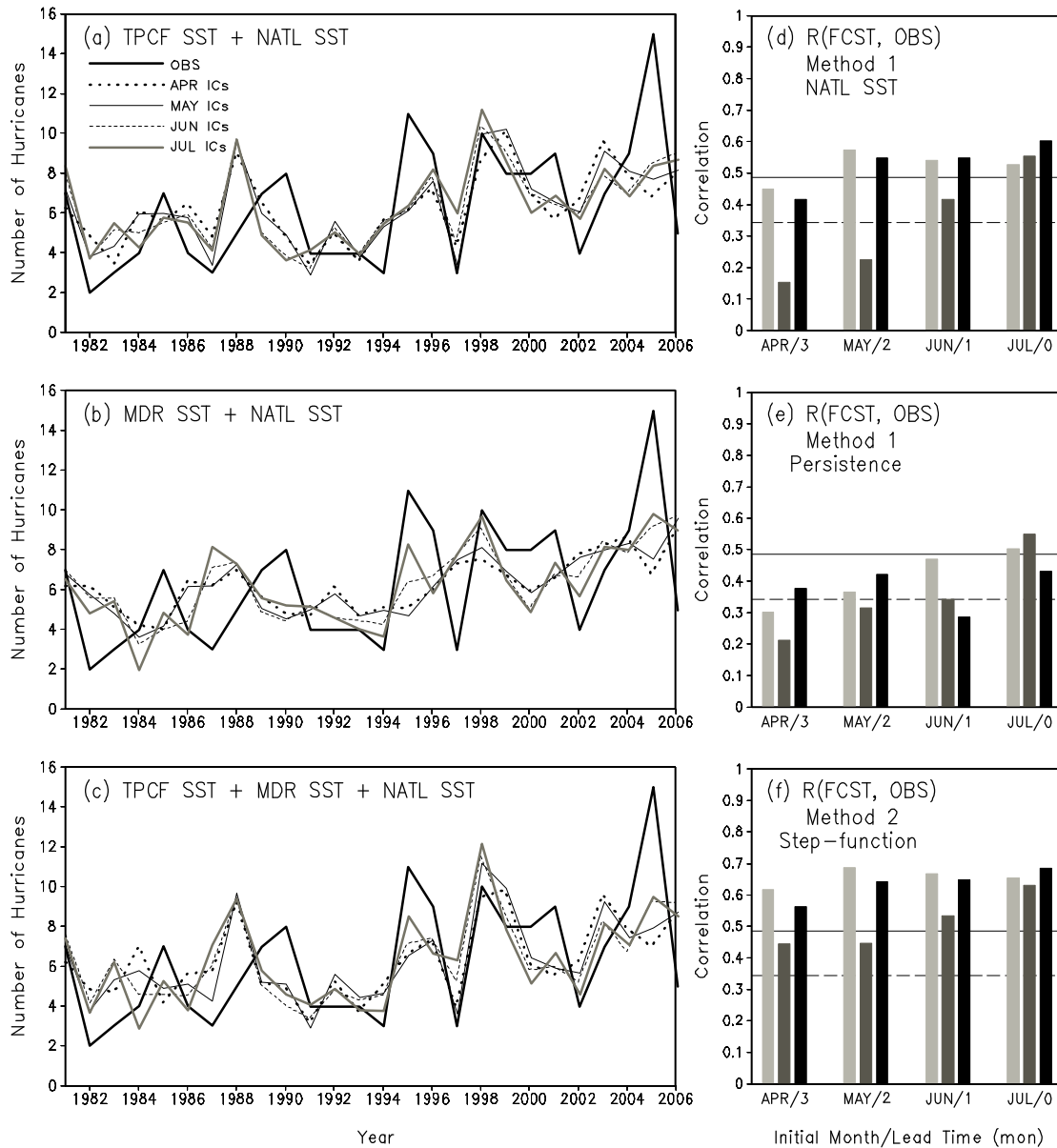


Fig. 9. (a)–(c) Observations (thick solid) and hindcasts of Atlantic hurricanes based on observed preseason NATL SSTs (Method 1) and CFS predicted ASO SSTs with April (thick dot), May (thin solid), June (dash), and July (thick solid grey) initial conditions, and correlations between the observations and hindcasts of the seasonal hurricanes for (d) Method 1, (e) also Method 1 but SST predictors from persisted anomaly forecasts and (f) Method 2, respectively. The hurricane hindcasts are based on ASO (a) TPCF SST, (b) MDR SST, and (c) both TPCF SST and MDR SST as the predictors. Light grey, grey and black bars in (d)–(f) indicate the correlations between observations and forecasts when using the TPCF SST (light grey), the MDR SST (grey) or both SSTs (black) as the predictors, respectively. The dash and solid lines in (d,e,f) indicate the 5% and 1% significance levels estimated by the Monte Carlo tests.

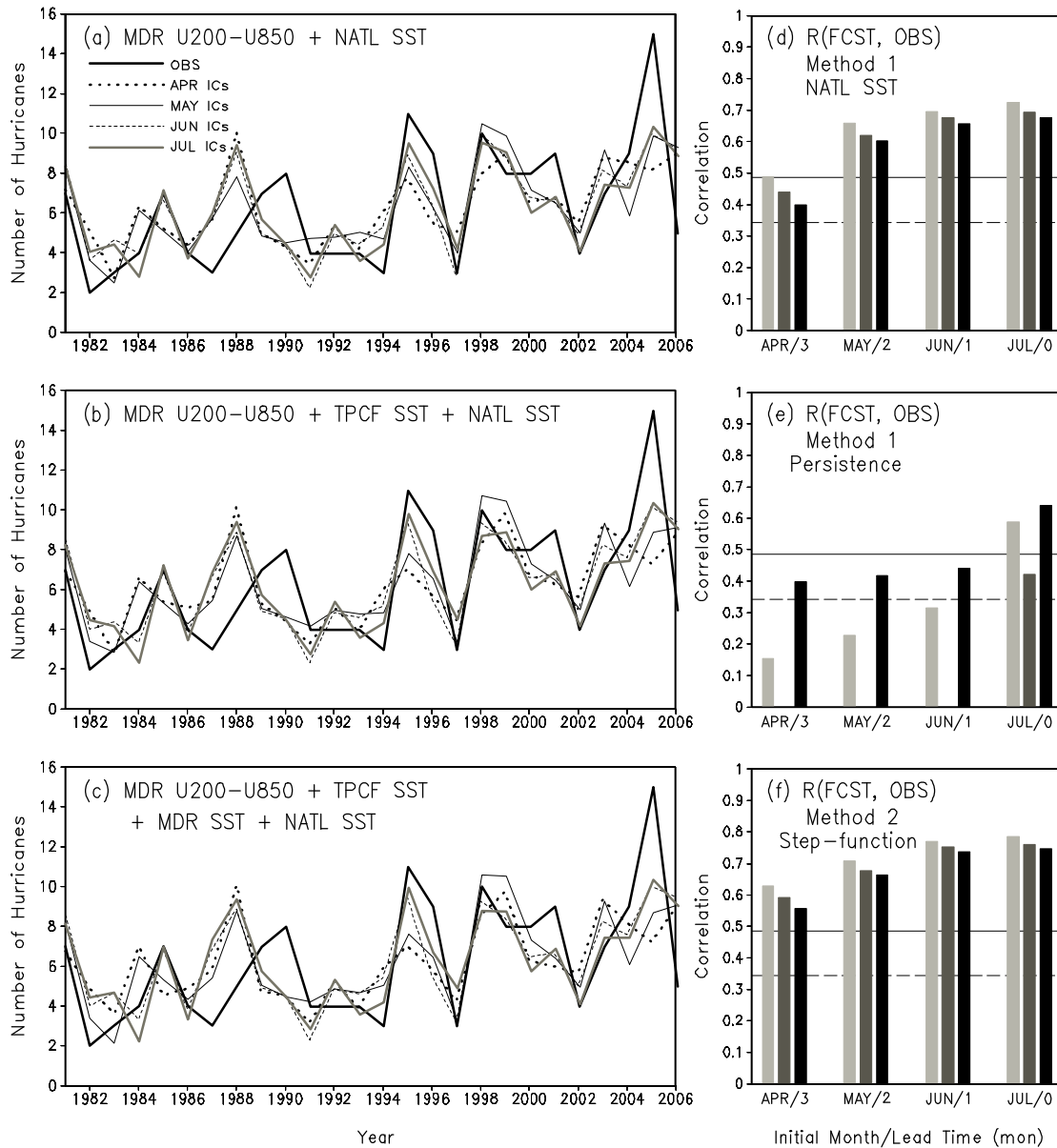


Fig. 10. Same as in Fig. 9 but for hurricane hindcasts using CFS predicted ASO (a) MDR vertical wind shear, (b) MDR wind shear and TPCF SST, and (c) MDR wind shear, TPCF SST and MDR SST as the predictors. Light grey, grey and black bars in (d)–(f) indicate the correlations between observations and hindcasts when using the MDR wind shear (light grey), MDR wind shear and TPCF SST (grey) and MDR wind shear, TPCF and MDR SSTs (black), respectively, for (d) Method 1, (e) Method 1 with predictors from persisted anomaly forecasts and (f) Method 2.